A FULLY AUTOMATED METHOD OF ASSOCIATING AXIAL SLICES WITH A DISC BASED ON LABELING OF MULTI-PROTOCOL LUMBAR MRI

*Jaehan Koh, Vipin Chaudhary**

University at Buffalo (SUNY)
Department of Computer Science and Engineering
Buffalo, NY 14260, USA
{jkoh,vipin}@buffalo.edu

Gurmeet Dhillon

Proscan Imaging of Buffalo
Williamsville, NY 14221, USA
gdhillon@proscan.com

ABSTRACT

In a clinical setting, sagittal magnetic resonance imaging (MRI) slices along with axial MRI slices are commonly examined to diagnose lower lumbar disorders. Alongside, scan lines by projecting axial slices onto sagittal slices are provided to show the relationship about which axial slice is associated with a particular disc, resulting in better diagnosing disc-related disorders by a radiologist. In this paper, we propose a method to accurately associate an axial MRI with the particular intervertebral disc in a pre-labeled sagittal lumbar region MRI. A statistical distance prior from multi-protocol MR images of 68 patients is used in labeling process to accommodate the variability of the distance among patients of different ages and gender. Experiments with 93 patient data including 465 lumbar discs show that our method can assign the class membership to scan lines with over 92% accuracy.

Index Terms— Scan Line, Association, MRI, Labeling, Localization, Lumbar Discs

1. INTRODUCTION

The 2002 National Health Interview Survey and National Ambulatory Medical Care Survey data showed that low back pain is the major cause of the physician visits across all age groups in the United States [1]. Accordingly, a huge amount of money and time is spent for obtaining accurate images and diagnosis. Recently, MRI is widely adopted in the diagnosis of lumbar spinal disorders including disc herniation, lumbar stenosis, and degenerative disc disease [2]. Although MRI takes long scan time and is costly, it has several advantages. MRI provides a high level of accuracy in capturing soft tissues of the body and allows radiologists to detect other problems such as bone tumors and infections of the spine. Also, it can image in any plane of the body. An MRI system generates two-dimensional pictures of the spine from any degree angles without the need of the patient's movement. Typically in a clinical environment, three-dimensional MR imaging is still unfeasible given cost and time. Instead, two-dimensional sagittal and axial slices are commonly employed. In this setting, intersecting scan lines are computed by projecting slices in one protocol onto the slices in another protocol, and are displayed in a viewer software along with scan images to provide the association information between slices in different protocols as in Fig. 1(a). However, the relationship information, other than the scan lines themselves, about which scan lines are associated with which discs is not given explicitly by the system. When there are several scan slices from multiple protocols, it gets complicated to associate a slice in one protocol with a slice in another protocol as in Fig. 1(b). Since a few axial slices are associated with one intervertebral disc, if we can provide the association information with a particular disc, a radiologist can diagnose diseases a lot quicker based solely on those slices, rather than moving through the whole set of slices. In this paper, we propose a fully automated method to accurately associate an axial MRI with intervertebral discs in pre-labeled sagittal lumber region MRI. A statistical distance prior from multi-protocol MRI of 68 patients are used in the labeling process to accommodate the variability of the distance among different patients of gender and ages.

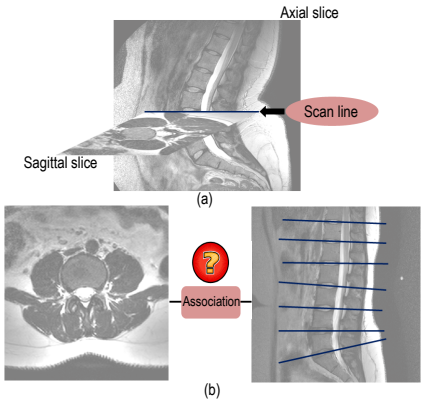

Fig. 1. How to determine the association of an axial slice to its related disc in the sagittal slice?

*The research was supported in part by a grant from NYSTAR and NSF.

2. RELATED WORK

Labeling assigns membership to each disc and vertebra while projection computes scan lines. Due to space limit, although there are several other papers on this topics, we included some of them that are most relevant to our work.

A lot of labeling work has been done along with localization. Chwialkowski *et al.* [3] presented a method to localize lumbar discs and spinal canal using the line of bisection from the center of gravity of two adjacent vertebrae. Weiss *et al.* [4] identified and labeled cervical, thoracic and lumbar vertebrae and discs using a semi-automated iterative technique. Corso *et al.* [5] proposed a two-level probabilistic model to localize and label lumbar discs and vertebrae robustly by integrating pixel-level information and object-level information. However, they did not account for the biological variability of the patients.

There have been many attempts to utilize scan planes. Derbyshire *et al.* [6] showed a scan-plane tracking system by automatically updating the imaging scan plane and by adaptively compensating for the subject motion. Yi *et al.* [7] implemented a six-degree-of-freedom hardware plane navigator to get visual feedback on the prescription by allowing to maneuver MRI scan planes in real-time. Despite an excellent ability to maintain static balance, it was not flexible to be used in diverse domains due to its fixed-size physical workspace. DiMaio *et al.* [8] proposed a general purpose image-based technique that tracks instruments and devices. The multi-planar imaging capabilities of the MRI were used to find the optimal device localization and visualization, allowing to dynamically servo the scan plane. However, their system required the MR-visible fiducial markers to control the closed-loop scan plane. These approaches tried to track scan planes but did not attempt to associate between them. The rest of the paper is organized as follows. In Section 3, our method of association is explained. Experimental results and discussion are given in Section 4. Finally Section 5 concludes our discussion.

3. METHOD

Our method involves three steps: (i) labeling and localization, (ii) scan line calculation and (iii) scan line association.

3.1. Problem Description

The proposed method associates scan lines calculated from projection of an axial slice onto a sagittal slice with intervertebral discs using the labeling and the localization algorithm we developed previously [9]. In the algorithm, an initial region of interest (ROI) is selected in the central region of a slice image. The spinal cord is extracted by considering intensity difference between a T2-weighted sagittal slice and a T1-weighted sagittal slice, and by a thresholding method. Then, an interpolation is applied to connect the cord pieces that might have been fallen apart due to severe spinal injury. After extracting the left boundary of the spinal column, the normals along the boundary are computed. Based on the normals, an intensity profile is obtained. Annulus fibrosus of the discs are extracted using the thresholds computed from the profile. In the post-processing step, incorrect disc center candidates are eliminated. The labeling is done from $L5 - S1$ since the $S1$ vertebra is usually more inclined with respect to the spinal cord.

The problem of labeling and localization is given as $LOC(I) = \{(x_i, y_i, z_i, l_i)\}$, where I is the set of MR images of patients comprising T1-weighted sagittal, T2-weighted sagittal and T2-weighted axial images. Here, (x_i, y_i, z_i) are the coordinates of each label in three dimensional space, and $l_i \in \{L1 - L2, L2 - L3, L3 - L4, L4 - L5, L5 - S1\}$ is a disc label in the low lumbar region. In addition, the problem of scan line association is defined as $SLC(I) = \{(SL_i, l_j)\}$, where SL_i is the set of scan lines obtained from the set of axial slices and the set of sagittal slices and i refers to the number of sagittal slices, respectively. Similarly to the problem of the labeling and localization, I is the set of MR images and l_j is a disc label.

3.2. Statistical Labeling and Localization

In this process, we model a probability distribution of distance between intervertebral discs to determine whether the distance between two adjacent intervertebral discs is changing significantly depending on the age and gender of the subjects. This accounts for the variability of the height of the lumbar vertebra and intervertebral discs due to morphological changes of vertebrae and discs. Clinically, the vertebral heights and intervertebral disc heights are used to identify deformities and patterns [10] [11]. In addition, this statistical distance model is used to improve labeling results by forcibly guaranteeing the the distance between two neighboring intervertebral discs as we see in Fig. 3.

To understand closely the relationship between the morphological changes of lumbar spine and the distance between adjacent intervertebral discs of patients according to different ages and gender, we statistically analyze the distance in terms of a box plot since it provides the rough shape and tendency of the distribution. For the calculation of the quartiles and median, we used MR image data from 68 male and female patients. Distances are computed for the following four different distance categories: $D(L4 - L5, L5 - S1)$ as the distance between the discs $L4 - L5$ and $L5 - S1$, $D(L3 - L4, L4 - L5)$ as the distance between the discs $L3 - L4$ and $L4 - L5$, $D(L2 - L3, L3 - L4)$ as the distance between the discs $L2 - L3$ and $L3 - L4$, and $D(L1 - L2, L2 - L3)$ as the distance between the discs $L1 - L2$ and $L2 - L3$. The constructed model is shown as a box plot in Fig. 2. Also, the quartile values and the median values for each distance category is given in Table 1. As we can see, there is no significant difference in distances across distance categories. According to the statistics, the distance between two adjacent interver-

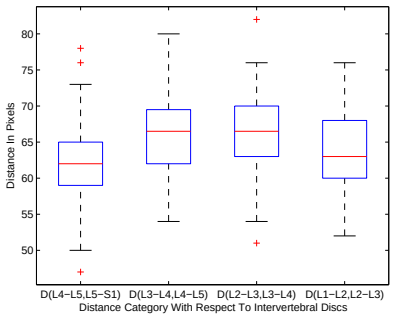

Fig. 2. A statistical model of the distance between intervertebral discs.

Distance Category	L. Quartile	Median	U. Quartile
$D(L4-L5, L5-S1)$	59	62	65
$D(L3-L4, L4-L5)$	62	66.5	69.5
$D(L2-L3, L3-L4)$	63	66.5	70
$D(L1-L2, L2-L3)$	60	63	68

Table 1. Quartiles (L. Quartile for lower quartile values and U. Quartile for upper quartile values) and median values of distances between adjacent intervertebral discs.

tebral discs is 64.5 pixels on average. This figure shows that the distance between two neighboring intervertebral discs is relatively constant across the lumbar discs regardless of the age and gender. This model is used as a standard reference to improve the performance of the labeling and localization algorithm.

3.3. Scan Line Calculation

In this step, we project an axial slice onto a sagittal slice thereby getting an intersecting line. Two-dimensional image coordinates of four corner points on the axial slice is augmented as $\begin{bmatrix} x & y & z \end{bmatrix}^\top = \begin{bmatrix} x & y & 1 \end{bmatrix}^\top$. Then, they are transformed into a voxel in the three-dimensional homogeneous coordinate system using a patient orientation and translation information stored in a Digital Imaging and Communications in Medicine (DICOM) header file. Specifically, the two-dimensional image slice is translated, scaled, rotated by the projective matrix $\mathbf{M}$ as follows: $\mathbf{M} = \mathbf{SRT_o}$ where $\mathbf{S} = \begin{bmatrix} \alpha & 0 & \mathbf{0} \\ 0 & \beta & \\ \mathbf{0} & & \mathbf{I_{2\times 2}} \end{bmatrix}$, $\mathbf{R} = \begin{bmatrix} \mathbf{dr_{3\times 1}} & \mathbf{dc_{3\times 1}} & \mathbf{ds_{3\times 1}} & \mathbf{0} \\ & \mathbf{0_{1\times 3}} & & 1 \end{bmatrix}$, $\mathbf{T_o} = \begin{bmatrix} \mathbf{I_{3\times 3}} & \mathbf{tr_{3\times 1}} \\ \mathbf{0_{1\times 3}} & 1 \end{bmatrix}$. Note that $\mathbf{I}$ means an identity matrix and all matrices are 4×4 matrices [12]. The scale matrix $\mathbf{S}$ comprises the horizontal and vertical scale factors, α and β, respectively. The rotation matrix $\mathbf{R}$ is determined by row, column, and slice direction cosines, $\mathbf{dr}, \mathbf{dc}$, and $\mathbf{ds}$, respectively. The translation matrix $\mathbf{T_o}$ specifies translation with respect to $x-, y-$ and $z-$axis (that is, $\mathbf{tr}$) and it moves the voxel to the origin. Then, each voxel is projected onto the two-dimensional sagittal slice according to the following equation: $ax + by + cz + d = 0$.

The projected point on the sagittal slice of each four corner points on the axial slice is obtained by finding the point that gives the shortest Euclidean distance from the point to the projected slice. Thus, if a voxel $P(x_1, y_1, z_1)$ in three-dimensional space is projected onto the sagittal slice, the corresponding voxel should be $Q(x_2, y_2, z_2)$ such that the vector $\overrightarrow{QP}$ is parallel to the surface normal of the sagittal slice and gives the smallest magnitude of the vector. With those voxels and projected end points on the sagittal slice, scan lines are obtained.

3.4. Scan Line Association

After the localization and labeling information $LOC(I)$ is determined, the set of scan lines SL_i is computed. Then, the association of scan lines are performed based on the distance of the center of each discs and each scan line. To be specific, the distance from each scan line to the center of all discs is calculated and the class membership of the line is given to the one that gives the smallest Euclidean distance as follows:

$$\underset{i}{\operatorname{argmin}}\ D(Cd_i, SL_j) \tag{1}$$

where D represent the distance, and SL_j is the set of scan lines. Here, Cd_i is the coordinates of the center of i-th discs that are the subset of $LOC(I)$. In this process, $LOC(I)$ is used as standard reference for assigning class membership.

4. EXPERIMENTS

The experiments are performed on a machine with Intel Xeon 2GHz Processor, and 4GB physical memory.

4.1. Image Data

MR image data are taken from 93 males and female patients of all ages ranging from 17 to 52 years. T2-weighted axial slices, T1-weighted sagittal slices and T2-weighted sagittal slices (TR = 3157 ms, TE = 100 ms, and flip angle = 90°) were scanned using a 3T Philips scanner. The resolution of each slice in MRI data is 512×512 pixels. 68 patients data are used for the distance model, and the remaining 25 patient data are used for the experiment. In addition, a total of 465 lumbar discs are used in the experiment.

4.2. Results and Discussion

Fig. 3 compares labeling and localization results of one using the statistical distance model (as in Fig. 3 (b)) against the other without the use of the model (as in Fig. 3(a)). Clearly, Fig. 3(b) shows the better results since it regulates inter-disc distances in accordance with the statistical distance model while Fig. 3(a) demonstrates an incorrect localization that happens in disc levels $L1-L2$ and $L2-L3$. We performed experiments using the statistical distance model in labeling and localization. Since the coordinates of discs serve as standard reference, if they are calculated incorrectly, a wrong class membership is assigned to a scan line. For example, if we

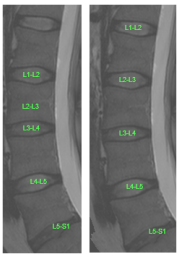

(a) (b)

Fig. 3. Comparison of localization results: (b) shows the improved localization results compared to (a).

Disc	$L1-L2$	$L2-L3$	$L3-L4$	$L4-L5$	$L5-S1$
Hit rate	80%	92%	96%	96%	96%

Table 2. Hit rate of the labeling and localization improved by a statistical distance model.

have a scan line passing through the disc $L2-L3$ in Fig. 3(b), that line will be associated with class $L1-L2$ instead of $L2-L3$, if the labeling is done as in Fig. 3(a). Table 2 shows the hit rate of labeling and localization based on the statistical distance model for all test cases. If the Euclidean distance of two discs is smaller than a threshold value τ, it forcibly spreads out the distance between two neighboring intervertebral discs using the median values computed from our model. Since the labeling and localization algorithm works from bottom (*i.e.*, $L5-S1$) to top (*i.e.*, $L1-L2$), the localization errors get accumulated as it goes up. That is why we get a low localization rate especially in the disc level $L1-L2$. On average, 92% of discs are localized and labeled correctly. If the labeling and localization are done correctly, all scan lines are associated correctly across all discs for the entire test data since the axial slices are taken along with the sagittal slices and the distance between the scan line and its associated disc is very small compared to the center of neighboring discs. Fig. 4 shows several association results.

5. CONCLUSIONS

In this paper, we propose a statistical method to generate scan lines between two slices in different protocols, *i.e.*, an axial slice and a sagittal slice, and associate them using the labeling algorithm and a statistical distance prior. The experimental results from 93 patient MRIs show that the scan lines are associated with 92% accuracy. These scan lines and their class labels help radiologists shorten their time for diagnosing several lumbar spine disorders.

6. REFERENCES

[1] R.A. Deyo, S. Mirza, and B.I. Martin, "Back pain prevalence and visit rates: estimates from U.S. national surveys, 2002," *Spine*, 2006.

[2] G.M. Weisz, S.T. Lamond, and P.N. Kitchener, "Magnetic resonance imaging in spinal disorders," *International Orthopaedics*, vol. 12, pp. 331–334, 1988.

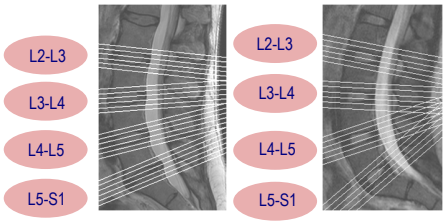

Fig. 4. Association results of scan lines where an axial slice is projected onto a sagittal slice.

[3] M.P. Chwialkowski, P.E. Shile, R.M. Peshock, D. Pfeifer, and R.W. Parkey, "Automated detection and evaluation of lumbar discs in MR images," *EMBC*, vol. 2, pp. 571–572, 1989.

[4] K. Weiss, J. Storrs, and R. Banto, "Automated spine survey iterative scan technique," *Radiology*, vol. 239, pp. 255–262, 2006.

[5] J.J. Corso, R.S. Alomari, and V. Chaudhary, "Lumbar disc localization and labeling with a probabilistic model on both pixel and object features," *MICCAI 2008*, pp. 202–210, 2008.

[6] J.A. Derbyshire, G. A. Wright, R.M. Henkelman, and R.S. Hinks, "Dynamic scan-plane tracking using MR position monitoring," *J. Magnetic Resonance Imaging*, vol. 8, pp. 924–932, 1997.

[7] D. Yi, J. Stainsby, and G. Wright, "Intuitive and efficient control of real-time MRI scan plane using a six-degree-of-freedom hardware plane navigator," *MICCAI 2004*, pp. 430–437, 2004.

[8] S.P. DiMaio, E. Samset, G. Fischer, I. Iordachita, G. Fichtinger, F. Jolesz, and C.M. Tempany, "Dynamic MRI scan plane control for passive tracking of instruments and devices," *MICCAI 2007*, vol. LNCS 4792, pp. 50–58, 2007.

[9] C. Bhole, S. Kompalli, and V. Chaudhary, "Context-sensitive labeling of spinal structures in MRI images," *SPIE Medical Imaging 2009*, pp. 803–806, 2009.

[10] Z. Shao, G. Rompe, and M. Schiltenwolf, "Radiographic changes in the lumbar intervertebral discs and lumbar vertebrae with age," *Spine*, vol. 27, no. 3, pp. 263–268, 2002.

[11] O. Sevinc, C. Barut, M. Is, N. Eryoruk, and A.A. Safak, "Influence of age and sex on lumbar vertebral morphometry determined using sagittal magnetic resonance imaging," *Annals of Anatomy*, vol. 190, pp. 277–283, 2008.

[12] M. Sonka, V. Hlavac, and R. Boyle, *Image Processing, Analysis, and Machine Vision*, Thompson Learning, 3 edition, 2008.